LIMNOLOGY and OCEANOGRAPHY

ASLO

Limnol. Oceanogr. 9999, 2021, 1–15

doi: 10.1002/lno.11766

Warming exacerbates the impact of nutrient enrichment on microbial functional potentials important to the nutrient cycling in shallow lake mesocosms

Lijuan Ren,[1] Yuanyuan Liu,[1] Torben L. Lauridsen,[2,3] Martin Søndergaard,[2,3] Boping Han,[1] Jianjun Wang [4], Erik Jeppesen,[2,3,5,6*] Jizhong Zhou,[7,8,9] Qinglong L. Wu [2,4*]

[1]Department of Ecology and Institute of Hydrobiology, Jinan University, Guangzhou, China
[2]Sino-Danish Centre for Education and Research, University of Chinese Academy of Sciences, Beijing, China
[3]Department of Bioscience, Aarhus University, Silkeborg, Denmark
[4]State Key Laboratory of Lake Science and Environment, Nanjing Institute of Geography and Limnology, Chinese Academy of Sciences, Nanjing, China
[5]Limnology Laboratory, Department of Biological Sciences and Centre for Ecosystem Research and Implementation, Middle East Technical University, Ankara, Turkey
[6]Institute of Marine Sciences, Middle East Technical University, Mersin, Turkey
[7]Institute for Environmental Genomics and Department of Microbiology and Plant Biology, School of Civil Engineering and Environmental Sciences, University of Oklahoma, Norman, Oklahoma
[8]Earth and Environmental Sciences, Lawrence Berkeley National Laboratory, Berkeley, California
[9]State Key Joint Laboratory of Environment Simulation and Pollution Control, School of Environment, Tsinghua University, Beijing, China

Abstract

Shallow lakes, the most numerous waterbodies on Earth, are susceptible to climate warming and nutrient enrichment whose effects on the microbial functional potentials are not yet fully understood, however. Here, we applied a microarray-based technology termed GeoChip 5.0 to investigate microbial functional genes at the beginning of April in shallow lake ecosystems simulated in mesocosms that have been undergoing nutrient enrichment and warming for 9 yr. Our results showed that warming exacerbated the impact of nutrient enrichment on microbial metabolic potentials and significantly elevated the microbial autotrophy potentials, carbon degradation potentials (e.g., starch, hemicellulose, cellulose, and chitin), and polyphosphate mobilization potentials. We also observed that warming enhanced the impacts of nutrient enrichment on microbial functional gene structure. The combination of warming and nutrient enrichment increased the deterministic effect from phytoplankton, causing higher interlinking of microbial functional genes involved in the carbon, nitrogen, phosphorus, and sulfur cycling in correlation-based networks. Overall, we propose that the joint effect of warming and nutrient enrichment promoted the autotrophic carbon supply and the heterotrophic carbon demand and changed the carbon fluxes in the experimental mesocosms.

The biosphere is in the midst of a pronounced warming trend. The Earth's surface temperature has increased by 0.76°C since 1850, and the temperature will expectedly have increased by another 1.1–6.4°C by the end of the 21st century (IPCC 2007). The increasing temperature alters the functioning of many ecosystems (Hoegh-Guldberg and Bruno 2010; Jeppesen et al. 2010; Woodward et al. 2010; Zhou et al. 2012; Guo et al. 2019). Shallow lakes, the most numerous waterbodies on Earth, are particularly vulnerable to the currently observed warming trends (Jeppesen et al. 2010; Kosten et al. 2011; Verpoorter et al. 2014). However, they are also highly vulnerable to human activities in their catchments, such as the nutrient input (Jeppesen et al. 2010). Organic carbon fluxes and nutrient cycling in the water columns of shallow lakes are mostly driven by microorganisms (Garcia et al. 2013; Ren et al. 2018). Changes in microbial functionality may affect the resilience of all other organisms and hence their ability to respond to climate change (Woodward et al. 2010; Kelly et al. 2019). Despite the crucial importance of microorganisms in climate warming biology, information is scarce on how climate warming and nutrient enrichments the

*Correspondence: qlwu@niglas.ac.cn (Q.L.W.); ej@bios.au.dk (E.J.)

Additional Supporting Information may be found in the online version of this article.

two most dominant factors, jointly affect the microbial functional structure and its potential feedback (Özen et al. 2013; Cavicchioli et al. 2019).

Previous evidence suggests that there is a combined effect of warming and nutrient enrichment on aquatic bacterial taxonomic (based on 16S rRNA gene sequencing) community composition (Ren et al. 2017), causing a dramatic change in the composition of bacterial communities toward increased percentages of cyanobacteria (Ren et al. 2017). However, changes in microbial composition do not always entail a functional shift due to microbial functional redundancy (Allison and Martiny 2008; He et al. 2012; Zhang et al. 2019). It is generally believed that the microbial community composition determined from 16S rRNA gene sequencing is less useful than functional traits for predicting biogeochemical properties, especially ecosystem functioning (Teeling et al. 2012; Escalas et al. 2019).

Functional traits are ecologically valuable parameters for understanding the assembly of microbial communities (Barberán et al. 2012), which may be affected by climate warming simply due to the influence of temperature on microbial biochemical kinetics (Brown et al. 2004). Moderate increases in temperature can result in high microbial metabolic rates (Christoffersen et al. 2006; Shurin et al. 2012; Özen et al. 2013), and these ultimately determine the biogeochemical processes involved in the nutrient cycling of carbon (C), nitrogen (N), phosphorous (P), and sulfur (S) (O'Connor et al. 2009; Yvon-Durocher et al. 2014). For instance, elevated temperatures can greatly influence the mobilization of phosphorus from mineral-bound and polyphosphate forms (Søndergaard et al. 2003; Bai et al. 2009). Warming may also increase greenhouse gas emissions with an amplifying effect over time (Yvon-Durocher et al. 2017; Davidson et al. 2018). In addition, climate warming may indirectly affect microbial functional traits due to changes in primary producers. Previous studies suggest that warming, especially when interacting with nutrient enrichment, can promote phytoplankton growth (Meerhoff et al. 2007; Posch et al. 2012; Rigosi et al. 2014). This results in the replacement of submerged plants by phytoplankton, which modifies not only the biological communities but also the biogeochemical processes of shallow pelagic ecosystems (Jeppesen et al. 2009). High phytoplankton productivity in warmer eutrophic shallow lakes (Flanagan et al. 2003; Feuchtmayr et al. 2009) may increase the coupling of phytoplankton–microorganism dynamics and promote changes in microbial functional structure and the functional potentials involved in the nutrient cycling of C, N, P, and S due to the increased energy available to support the coexistence of multiple microbial functional traits (Bell et al. 2005; Litchman et al. 2015; Kiersztyn et al. 2019).

Although climate warming and nutrients affect microbial functional traits, the current knowledge regarding this relationship is insufficient. This is mainly due to the difficulty of obtaining reproducible and quantitative functional data at a community-wide level. High-throughput sequencing and microarrays are the commonly used technologies describing the functional compositions of microbial communities. Compared with the open-format technologies of high-throughput sequencing, such as genomic and metagenomic tools, the main limitations of the closed-format microarray technology like GeoChip-based functional gene arrays are that they prevent discovery of new genes, pathways, and taxa because all molecules used for designing the querying devices are known (Roh et al. 2010; Zhou et al. 2012). However, microarray technology is a useful method for routine studies of selected target sequences (He et al. 2012; Suenaga 2012). This "targeted metagenomics" approach is an effective means to understand the content and composition of genes for key ecological processes, such as C, N, P, and S utilization by microbial communities (e.g., Wang et al. 2009; Zhou et al. 2012). In this study, we used GeoChip-based functional gene arrays to examine microbial functional gene structure in outdoor mesocosms in Central Jutland, Denmark. These mesocosms simulate shallow lake systems under two nutrient regimes (oligotrophic and eutrophic) and two temperature scenarios, one acting as control and the other being heated according to the Intergovernmental Panel on Climate Change's climate scenario (IPCC) A2 + 50% with temperatures 4–5°C higher than the ambient (Liboriussen et al. 2005). We hypothesized that: (1) warming itself may alter the microbial metabolic potentials involved in nutrient cycling; (2) warming may also exacerbate the impact of nutrient enrichment on microbial functionality, and there is a joint effect between nutrient enrichment and warming; and (3) the changed metabolic potentials for nutrient cycling processes may affect ecosystem nutrient fluxes, creating a microbial feedback to climate change.

Methods

Mesocosm experiment

The mesocosm experiment was initiated in August 2003 in Lemming, Central Jutland, Denmark (56°14′N, 9°31′E). A detailed description of the mesocosms and the experimental setup can be found in Liboriussen et al. (2005). In our study, we selected 16 fully mixed, outdoor, flow-through mesocosms (diameter 1.9 m, water depth 1 m, retention time $\sim$ 2.5 months) combining two temperature scenarios (ambient temperature and warming simulating the IPCC A2 + 50% with temperatures 4–5°C higher than the ambient) and two nutrient levels with four replicates (Liboriussen et al. 2005). Nutrients were added weekly as Na_2HPO_4 and $Ca(NO_3)_2$ solutions to half of the mesocosms (dose: 2.7 mg P m^{-3} d^{-1} and 27.1 mg N m^{-3} d^{-1}), while the rest of the mesocosms remained unenriched. Macrophytes (*Elodea canadensis* Michx and *Potamogeton crispus* Linnaeus) were present in all nutrient-control mesocosms, while the enriched mesocosms were dominated by phytoplankton and filamentous algae and had sparse or no vegetation. Here, the treatments are termed as

follows: ambient temperature, unenriched (control); enhanced warming (A2 + 50%), unenriched (EW); ambient temperature, nutrient-enriched (NE); and enhanced warming (A2 + 50%), nutrient-enriched (NE and EW).

Sampling and chemical analyses

Sampling was conducted as described in detail by Ren et al. (2017). In brief, we collected 8 L pooled water samples from three uniformly distributed sites in each of the 16 mesocosms using a 1-m long tube water sampler that integrated the whole water column (twice on 02 April 2012). Approximately 400–500 mL of the collected water was used for microbial analysis and was filtered through 0.2-μm isopore filters (Millipore, Billerica, Massachusetts, U.S.A.). The filters were stored at −20°C until further analysis.

Water turbidity, chlorophyll *a* (Chl *a*), phosphate (PO_4^{3-}-P), nitrate (NO_x^--N), dissolved organic carbon (DOC), and total organic carbon (TOC) were analyzed according to standard methods (Søndergaard et al. 1990). Bacterial production rates were estimated using the Tritiated Thymidine incorporation method (Fuhrman and Azam 1982). The measurements and values of water temperature (*T*), dissolved oxygen (DO) levels, total phosphorus (TP), total nitrogen, plant abundance estimated as percent volume inhabited, gross primary productivity (GPP), ecosystem respiration (ER), and net primary productivity (NPP) in the mesocosms were shown as in the recent study by Ren et al. (2017).

DNA extraction and GeoChip analysis

DNA extraction was performed as in Ren et al. (2017). Briefly, whole microbial DNA was extracted (Wu et al. 2007) and purified using the Wizard DNA clean-up kit (Promega, Madison, Wisconsin, U.S.A.). GeoChip 5.0 was used for analyzing DNA samples, including more than 60,000 oligonucleotide probes and covering hundreds of gene families involved in the cycling of carbon, nitrogen, phosphorus, and sulfur (Yan et al. 2015). For each sample, DNA (500 ng) was labeled with the fluorescent dye Cy-3 (GE Healthcare, California, U.S.A.) by random priming (Shi et al. 2019). Labeled DNA was purified with a QIAquick purification kit (Qiagen, California, U.S.A.) and then dried in a SpeedVac (Thermo Savant, New York, U.S.A.). The dried and labeled DNA was resuspended in 42 μL of hybridization solution, which included 1 × HI-RPM hybridization buffer, 1 × CGH blocking agent, 0.05 $\mu g\,\mu L^{-1}$ Cot-1 DNA, 10 pmol L^{-1} universal standard, and 10% formamide (final concentrations). After complete mixing, the solution was denatured at 95°C for 3 min and kept at 37°C until hybridization. Hybridizations were performed at 67°C for 24 h with a rotation of 20 rpm in a hybridization oven. Scanned images of hybridized GeoChips were converted and extracted by using Agilent Feature Extraction 11.5 software (Agilent Technologies, California, U.S.A.).

Data preprocessing

Raw data were uploaded to the microarray analysis pipeline (http://ieg.ou.edu/microarray/) and analyzed as previously described (Ren et al. 2018). In brief, the following steps were performed: (1) spots with a signal-to-noise ratio less than 2 were removed due to poor quality; (2) for each sample, intensities plus 1 were transformed to logarithms and divided by mean signal intensity; (3) microbial metabolic potentials were further assessed by the relative signal intensity, which was normalized for the number of probes per sample (Chan et al. 2013).

Correlation-based network analysis

The microbial gene groups showing significant differences in metabolic potentials under the different warming and nutrient treatments were selected for correlation-based network construction. A Spearman correlation matrix between genes was calculated based on the relative gene abundances. To reduce the bias of correlation coefficients, only genes detected in at least 12 out of 16 samples were used for network construction. Subsequently, all possible Spearman rank correlations between genes across sampling mesocosms and the corresponding *p* values were calculated. We considered a valid correlation event to be robust if the absolute value of the Spearman correlation coefficient was > 0.6 and statistically significant at $p < 0.01$ based on method- and edge-specific permutations and bootstrap score distributions with 1000 iterations. Calculations were carried out using the Cytoscape plugin CONET (http://psbweb05.psb.ugent.be/conet/; Faust and Raes 2012). We generated subnetworks for each treatment from meta-community networks by preserving genes presented in all mesocosms involved in each treatment using subgraph functions in BioNet packages. The subnetworks were simplified by deleting the repeated edges using the simplify command in the igraph package in R. The new subnetworks in each warming and nutrient treatment were further visualized in ggplot2 packages. The Erdös–Rényi random network having the same nodes, edges, and degrees as the observed subnetwork was calculated using the implemented tool Network Randomizer, version 1.1.3. The topology of both the observed subnetworks and the corresponding random networks was calculated by the implemented tool network analyzer of Cytoscape (Assenov et al. 2008).

In a network, scale free means that most of the genes are connected to a low number of neighbor genes and that a small number of high-degree genes show high connectivity to the network. Degree indicates the number of links that a gene has to other genes in a network. Clustering coefficient represents that the degree to which genes in a network tends to cluster together. Density is the number of links that a gene has divided by the total possible links that a gene could have in a network. Connectivity is the minimum number of genes or links that need to be removed to separate the remaining genes into isolated subgraphs. Shortest path length represents the

shortest distance between any two nodes. Heterogeneity of a network means the heterogeneity among the number of edges maintained by each node. Component is where no connections exist between the genes of the different components in a network.

The relationships between the key functional genes and environmental and ecosystem metabolism factors were also investigated by correlation network analysis using the Cytoscape plugin CONET. The subnetworks of nodes (genes) having significant correlations with the environmental factors (Spearman correlation coefficient > 0.6, $p < 0.01$) were also generated using the subnetwork command in the BioNet package in R. The subnetworks were further simplified via the simplify command in the igraph in R and visualized by Cytoscape with a preferred layout.

Statistical analyses

Using the microarray analysis pipeline (http://ieg.ou.edu/microarray/), one-way ANOVA tests followed by post hoc comparisons were performed to determine significant differences in the relative signal intensity of each functional gene category and certain subcategories and in environmental characteristics under different warming and nutrient treatments. The evolutionary history of microorganisms carrying the rubisco gene was inferred by a neighbor-joining method with the Poisson correction method (Zuckerkandl and Pauling 1965) in MEGA X (Kumar et al. 2018). The relative signal intensities of the significantly different phylogenetic groups under different warming scenarios and nutrient conditions were depicted in a heat map with the pheatmap package in the R statistical computing environment (http://www.r-project.org).

A detrended correspondence analysis (DCA) and permutational multivariate analysis of variance (PERMANOVA) using distance matrices were performed to assess the effects of the different treatments on the changes in microbial functional gene structure using the vegan package (Legendre and Legendre 2012) in R. In the different treatments, significant differences in the relative signal intensity of all detected 37,138 genes were tested using differential expression analysis based on the negative binomial distribution in the R DESeq2 package (Love et al. 2014). Relationships between functional community composition and environmental factors were determined by the Mantel statistic with 999 permutations and canonical correlation analysis (CCA) with an automatic stepwise model using permutation tests in the R vegan package. The models in CCA were validated by ANOVA. To uncover the relative importance of deterministic and stochastic processes in shaping the microbial functional gene compositions, null-model analysis was performed, where the data matrix of microbial functional gene compositions was randomized using an independent swap algorithm in the R picante package. This randomized process was replicated 999 times to obtain 999 null compositions of each observed community. The standardized effect size of the Jaccard dissimilarity index (SES.Jaccard) and Bray-Curtis dissimilarity index (SES.Bray-Curtis) was estimated as the differences in beta diversity between the observed community compositions and the mean value of the 999 null community compositions divided by the standard deviation of the beta diversity in the 999 null community compositions. If SES.Jaccard/SES.Bray-Curtis is close to zero, the variations of microbial functional gene compositions are most likely driven by stochastic processes; however, if SES.Jaccard/SES.Bray-Curtis is far from zero, the relative importance of deterministic processes increases in microbial functional gene assembly.

Results

Shifts in the microbial metabolic potentials

In total, 37,138 genes were detected, including those involved in important biogeochemical processes such as C, N, P, and S utilization (Supporting Information Table S1). We found that compared with the control, neither warming nor nutrient enrichment alone had a significant effect on the metabolic potential of the microbes for autotrophic carbon fixation (Supporting Information Fig. S1, $p > 0.05$ in both cases), but their combination significantly increased the metabolic potential for autotrophic carbon fixation ($p < 0.05$, Supporting Information Fig. S1). In contrast to the reductive acetyl-CoA pathway, the metabolic potential for the Calvin-Benson-Bassham cycle (RuBisCo: rubisco, Supporting Information Table S1) was significantly increased by the joint effect of warming and nutrients (Fig. 1c[i], $p < 0.05$). Among the rubisco genes, 9 type IA genes, 7 type IC genes, and 4 type II genes increased significantly in the treatment combining warming and nutrient enrichment (Supporting Information Fig. S2, $p < 0.05$ in all cases). The metabolic potential for acetogenesis (i.e., tetrahydrofolate formylase: FTHFS in the Wood-Ljungdahl pathway), methanogenesis (methyl coenzyme m reductase A: mcrA), and methane oxidation (soluble methane monooxygenase: mmoX and particulate form methane monooxygenase: pmoA) showed no significant changes in the treatments with warming, nutrient enrichment, or joint warming and nutrient enrichment ($p > 0.05$ in all cases, Fig. 1a–c).

Regarding the overall carbon degradation potential, we found the carbon degradation potential was significantly higher in both the pure warming and the pure nutrient enrichment treatments than in the control ($p < 0.05$ in all cases, Supporting Information Fig. S1). However, compared with the treatments of pure warming and pure nutrient enrichment, an enhanced carbon degradation potential was observed under the joint effect of warming and nutrient enrichment ($p < 0.05$ in all cases, Supporting Information Fig. S1). In the specific carbon sources such as starch, hemicellulose, cellulose, and chitin, the microbial degradation potentials increased significantly in the pure nutrient-enriched treatment for hemicellulose (xylanase, $p < 0.05$, Fig. 1e).

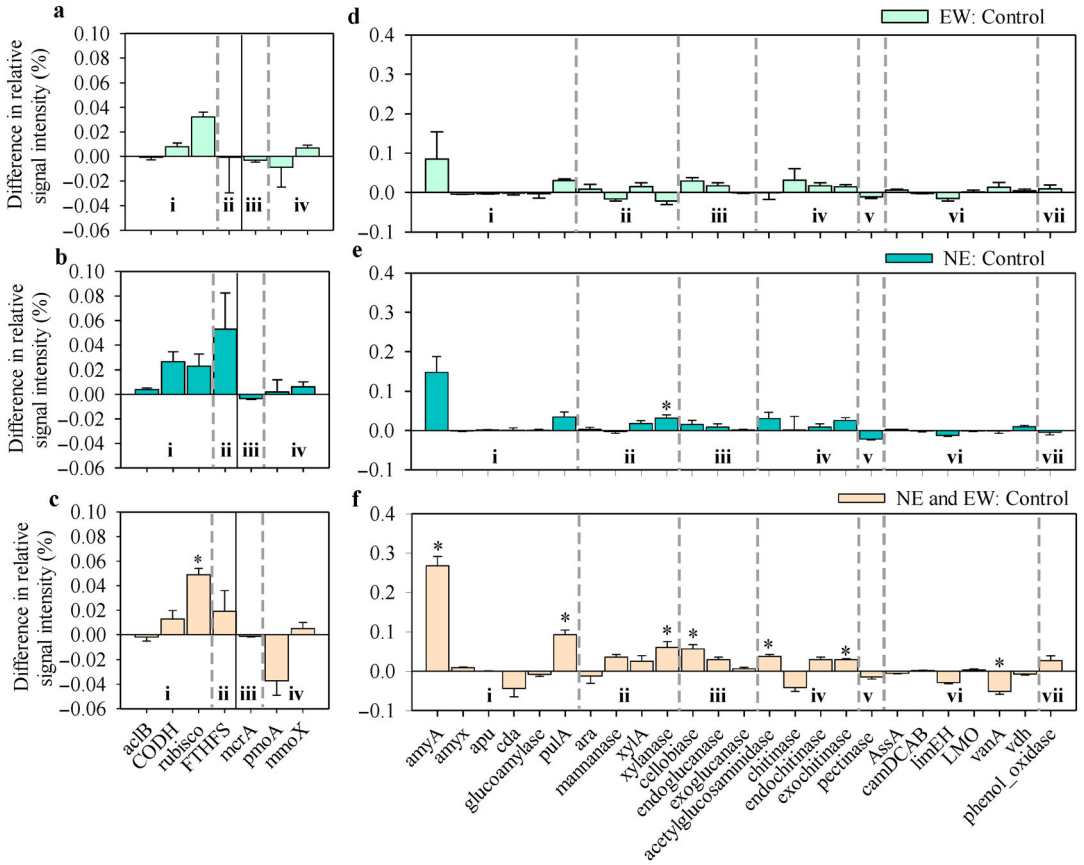

Fig. 1. Differences in the microbial metabolic potentials (characterized as the relative signal intensity) for carbon cycling between different warming and nutrient treatments and the control (i.e., ambient temperature and unenriched treatment). (**a**–**c**) Subcategories of carbon cycling genes (i: autotrophy, ii: acetogenesis, iii: methanogenesis, and iv: methane oxidation); (**d**–**f**) Each subcategory of carbon degradation (i: starch, ii: hemicellulose, iii: cellulose, iv: chitin, v: pectin; vi: aromatic, and vii: lignin). The full names of the enzyme/protein encoded by the functional genes are shown in Supporting Information Table S1. The treatments are termed as follows: ambient temperature, unenriched (control); enhanced warming (A2 + 50%), unenriched (EW); ambient temperature, nutrient-enriched (NE); and enhanced warming (A2 + 50%), nutrient-enriched (NE and EW). EW: Control, NP: Control, and NE and EW: Control mean the metabolic potential differences of EW and control, NE with control, and NE and EW with control, respectively. *$p < 0.05$.

Significantly higher carbon degradation potentials for starch (alpha-amylase: amyA and pullulanase: pulA), cellulose (cellulose: cellobiase), and chitin (acetylglucosaminidase and exochitinase) metabolism were only observed in the combined warming and nutrient treatment ($p < 0.05$ in all cases, Fig. 1f) and not in the pure warming or the pure nutrient-enriched treatments ($p > 0.05$ in all cases, Fig. 1d,e).

For N cycling, the major difference between the functional groups was ammonification (Supporting Information Fig. S1a, b and c [ii]). Compared with the control, the metabolic potential of ammonification significantly decreased both in the nutrient-enriched treatment (primarily urease: ureC; $p < 0.05$, Supporting Information Fig. S1 and Fig. 2b[ii]) and in the joint treatment of warming and nutrient enrichment (primarily glutamate dehydrogenase: gdh and ureC; $p < 0.05$ in both cases, Supporting Information Fig. S1 and Fig. 2c[ii]). Additionally, for P cycling, we found that warming and nutrient enrichment exerted a combined effect on polyphosphate biosynthesis and degradation as indicated by the increased relative signal intensity of polyphosphate kinase (ppk) and exopolyphosphatase (ppx). However, the joint effect of warming and nutrient enrichment was only significant on ppx ($p < 0.05$, Fig. 2d–f) and not on ppk ($p > 0.05$, Fig. 2d–f). Finally, the functional ability of sulfide oxidation (provided primarily by flavocytochrome c sulfide dehydrogenase: fccAB) also increased in the S cycling due to the joint effect of warming and nutrient enrichment ($p < 0.05$, Fig. 2g–i).

Shifts in microbial functional gene structure and assembly mechanisms

Our results revealed that there was no significant effect of warming on the overall microbial functional gene structure without nutrient enrichment (pairwise PERMANOVA, Jaccard dissimilarity: $p > 0.05$, Bray-Curtis dissimilarity: $p > 0.05$; Table 1, Supporting Information Table S2, Fig. 3a,b) and only a modest effect of an enhanced nutrient level at ambient

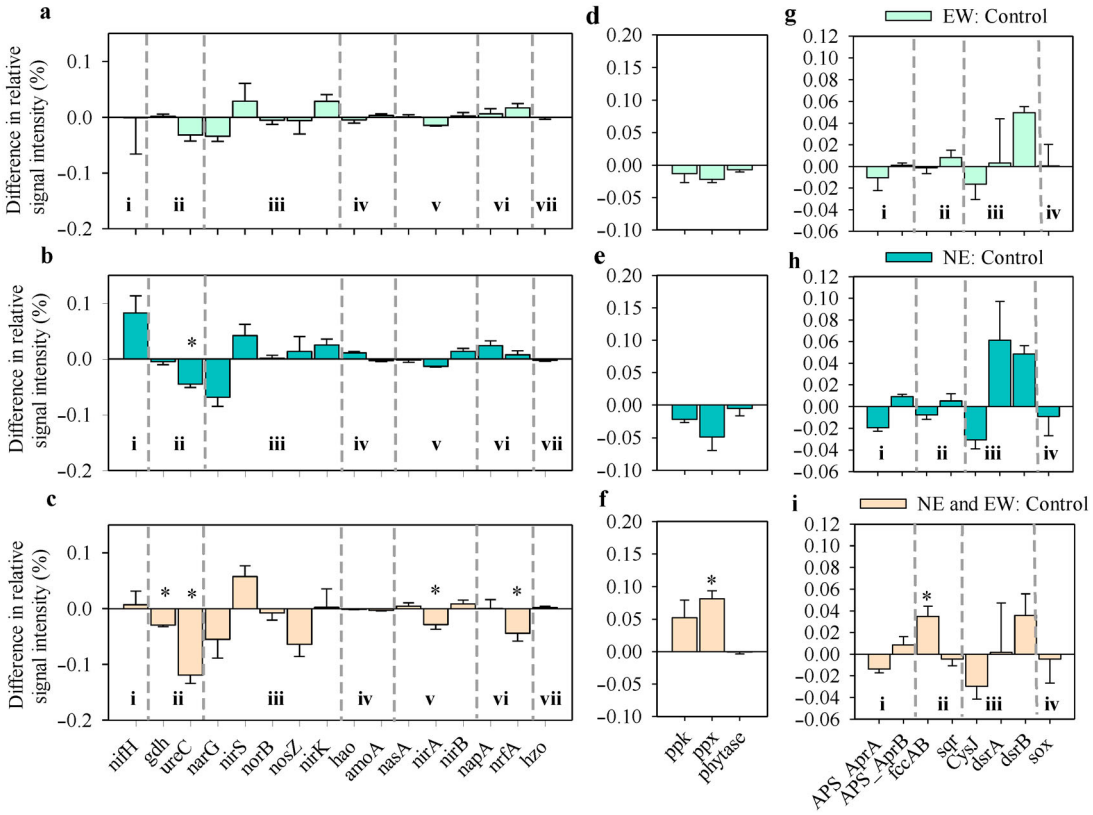

Fig. 2. Differences in the microbial metabolic potentials (characterized as the relative signal intensity) for certain biogeochemical cycling processes in different warming and nutrient treatments. (**a**–**c**) Each subcategory of nitrogen cycling, i: nitrogen fixation, ii: ammonification, iii: denitrification, iv: nitrification, v: assimilatory N reduction, vi: dissimilatory N reduction, and vii: anammox; (**d**–**f**) Each subcategory of phosphorus cycling; (**g**–**i**) Each subcategory of sulfur cycling, i: adenylyl sulfate reductase, ii: sulfide oxidation, iii: sulfite reduction, and iv: sulfur oxidation. The full names of the enzyme/protein encoded by the functional genes are given in Supporting Information Table S1. The treatments are termed as follows: ambient temperature, unenriched (control); enhanced warming (A2 + 50%), unenriched (EW); ambient temperature, nutrient-enriched (NE); and enhanced warming (A2 + 50%), nutrient-enriched (NE and EW). EW: Control, NE: Control, and NE and EW: Control mean the metabolic potential differences of EW with control, NE with control, NE and EW with control, respectively. *$p < 0.05$.

Table 1. Pairwise PERMANOVA of microbial functional gene structure based on Jaccard/Bray-Curtis dissimilarity.

	Jaccard dissimilarity		Bray-Curtis dissimilarity	
Groups	***F***	***p* value**	***F***	***p* value**
Whole	2.778	0.001**	3.611	0.002**
Control vs. EW	1.491	0.236	1.374	0.229
Control vs. NE	1.695	0.081	1.526	0.091
Control vs. NE and EW	3.049	0.011*	4.547	0.001**
EW vs. NE	1.871	0.005**	1.641	0.001**
EW vs. NE and EW	3.889	0.001**	5.675	0.012*
NE vs. NE and EW	4.208	0.001**	6.022	0.001**

*$p < 0.05$; **$p < 0.01$.

temperature compared with the control treatment (pairwise PERMANOVA, Jaccard dissimilarity: $p < 0.1$, Bray-Curtis dissimilarity: $p < 0.1$; Table 1, Supporting Information Table S2, Fig. 3a,b). However, warming exacerbated the impact of nutrient enrichment on the microbial functional gene structure, and there was a joint effect of nutrient enrichment and warming that significantly changed the overall microbial functional gene structure compared with the control treatment (Jaccard dissimilarity: $p < 0.05$, Bray-Curtis dissimilarity: $p < 0.05$; Table 1, Supporting Information Table S2, Fig. 3a,b).

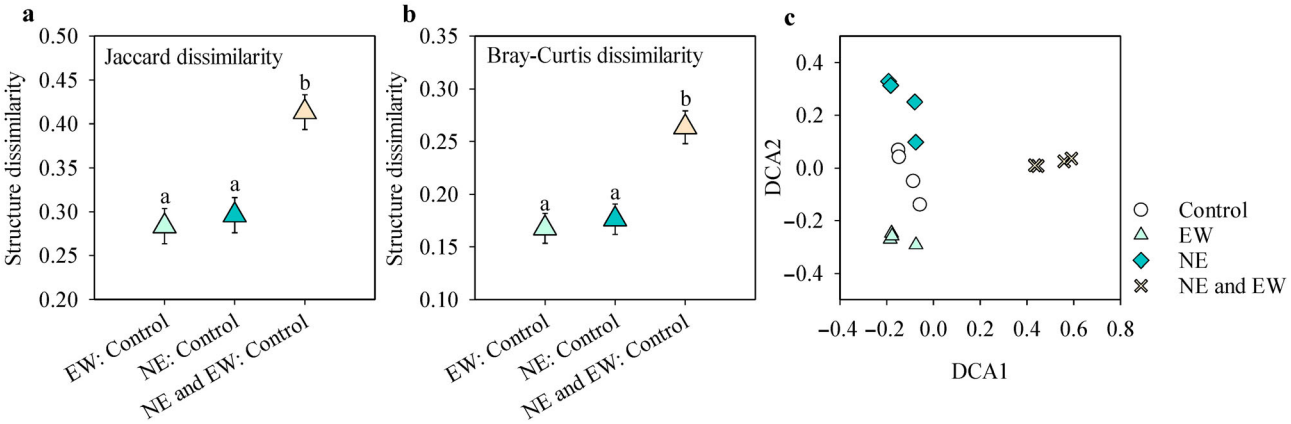

Fig. 3. Structural dissimilarity of the overall microbial functional genes between different warming and nutrient treatments and the controls (**a**: based on Jaccard's dissimilarity; **b**: based on Bray-Curtis dissimilarity) and the microbial overall functional gene structure in response to warming and nutrients as identified by DCA (**c**). The treatments are termed as follows: ambient temperature, unenriched (control); enhanced warming (A2 + 50%), unenriched (EW); ambient temperature, nutrient-enriched (NE); and enhanced warming (A2 + 50%), nutrient-enriched (NE and EW). EW: Control, NE: Control, and NE and EW: Control mean the structure dissimilarity of EW with control, NE with control, NE and EW with control, respectively. Significant ($p < 0.05$) differences among groups are indicated by different alphabetic letters above the bars.

The effects of warming and nutrient enrichment on the functional gene structure of microbial communities were also confirmed by DCA (Fig. 3c). Similar results were observed in the functional gene structure of the subcategories of C, N, P, and S cycling (Supporting Information Table S3 and Fig. S3).

Among the detected 37,138 genes, 9619 genes were found to differ significantly in relative signal intensity under the four different warming and nutrient treatments ($p < 0.05$ in all cases). Thus, our study revealed that, besides the combined effect of warming and nutrient enrichment (Jaccard dissimilarity: $p < 0.05$, Bray-Curtis dissimilarity: $p < 0.05$, Supporting Information Table S4, Fig. S4), pure warming and pure nutrient enrichment also had a significant influence on the microbial functional gene structure of these 9619 genes (Jaccard dissimilarity: $p < 0.05$ in both cases, Bray-Curtis dissimilarity: $p < 0.05$ in both cases; Supporting Information Table S4, Fig. S4). However, the impacts of both pure warming and pure nutrient enrichment on the microbial functional gene structure were exacerbated 0.5 times to 0.9 times by the joint effect of warming and nutrient enrichment (Supporting Information Fig. S4).

The null model analysis revealed that both SES.Jaccard and SES.Bray-Curtis under the combined treatment of warming and nutrient enrichment were significantly lower than those under the other treatments and far below zero ($p < 0.05$ in all cases, Fig. 4a,b), indicating that the relative importance of deterministic assembly processes increased under the combined effect of warming and nutrient enrichment. This finding was further confirmed by network analysis where most of the microbial functional genes in the different warming and nutrient networks tended to be copresent rather than randomly distributed. Moreover, the four functional gene networks obtained for the different warming and nutrient treatments were scale free ($R^2 > 0.8$) (Table 2). In comparison with the other treatments, warming and nutrient enrichment in combination decreased the heterogeneity, components, and path length of the microbial network but increased the network clustering, neighborhood connectivity, centralization, density, and average degree (Table 2).These changed network topological properties indicated that compared with other treatments, the interlinking of microbial functional genes involved in the C, N, P, and S cycling obviously increased when warming and nutrient enrichment were combined.

Microbial functional gene structure related to environmental factors

Among all environment factors and ecosystem metabolisms (Supporting Information Table S5 and Table 2 in Ren et al. 2017), we observed that the overall microbial functional gene structure was best explained by Chl *a*, an indicator for phytoplankton abundance (Supporting Information Fig. S5), followed by the concentrations of TOC, TP, DOC, ER, and DO (Supporting Information Fig. S5). Consistent results were found regarding the functional structure of the total key genes involved in C (i.e., rubisco, amyA, pulA, xylanase, cellobiase, acetylglucosaminidase, exochitinase, and vanillate demethylase: vanA), N (i.e., gdh, ureC, nitrite reductase: nirA, and ammonia-forming cytochrome c nitrite reductase: nrfA), P (i.e., ppx), and S cycling (i.e., fccAB) (Supporting Information Fig. S5) and the functional structure of the specific gene groups, including amyA, vanA, gdh, and nirA (Supporting Information Fig. S5). Water temperature was the key factor in determining the functional structure of some specific gene groups such as exochitinase, cellobiase, and nirA although it had insignificant effects on the overall functional gene structure (Supporting Information Fig. S5).

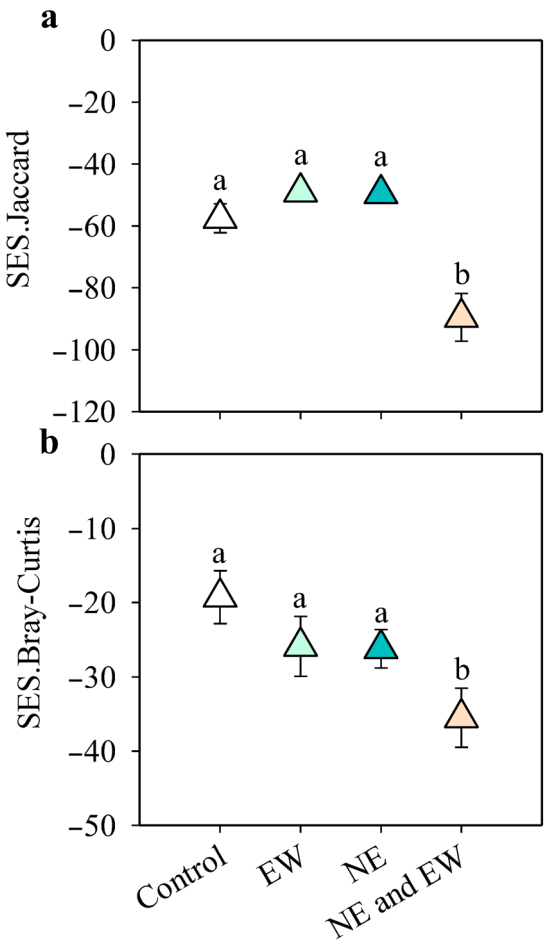

Fig. 4. The standardized effect size of the Jaccard dissimilarity index (SES.Jaccard, **a**) and the standardized effect size of the Bray-Curtis dissimilarity index (SES.Bray-Curtis, **b**) in response to warming and nutrients in the shallow lake mesocosms. The treatments are termed as follows: ambient temperature, unenriched (control); enhanced warming (A2 + 50%), unenriched (EW); ambient temperature, nutrient-enriched (NE); and enhanced warming (A2 + 50%), nutrient-enriched (NE and EW). Significant ($p < 0.05$) differences among treatments are indicated by different alphabetic letters above the bars relative to post hoc comparisons.

The correlation network of the key functional genes and environmental factors revealed that 31% of the detected genes/nodes in the network correlated significantly with the investigated environmental factors (Fig. 5a). The association network indicated that among all of the environmental variables included in our study, Chl *a* had the most links with the key genes involved in the C, N, P, and S cycling, followed by TOC, temperature, TP, GPP, and ER (Fig. 5b). A higher percentage of exclusive links with environmental factors was observed in the relative signal intensity (metabolic potentials) of the genes vanA (66%), gdh (52%), ureC (66%), nirA (61%), and nrfA (65%) than in those of rubisco (47%), pulA (27%), xylanase (38%), cellobiase (37%), acetylglucosaminidase (38%), exochitinase (0%), and fccAB (15%). By using the automatic stepwise model with permutation tests, canonical correspondence analysis (CCA) revealed that water Chl *a*, ER, temperature, and DO were the key variables that significantly explained the microbial functional gene structure ($F = 2.21$, $p < 0.01$; Supporting Information Fig. S6).

Discussion

The central role and global importance played by microorganisms in climate change biology have recently been emphasized (Cavicchioli et al. 2019). Microorganisms can affect climate change (including the production and consumption of greenhouse gases) and can also be altered by climate change and human activities. However, our knowledge about the interactive effects of climate warming and nutrient enrichments on microbial functional ecology in shallow lake ecosystems is scarce. In this study conducted at the beginning of April, we found that warming exacerbated the impact of nutrient enrichment on the microbial functional structure. Warming and nutrient conditions also had significant effects on microbial metabolic potentials (Fig. 6). We found that addition of nitrogen and phosphorus at ambient temperature had significant effects, such as carbon degradation (e.g., hemicellulose) and ammonification (Fig. 6), on microbial metabolic potentials. However, warming enhanced the nutrient enrichment impacts on microbial metabolic potentials that significantly elevated microbial autotrophy potentials, carbon degradation potentials (e.g., starch, hemicellulose, cellulose, and chitin), and polyphosphate mobilization potentials (Fig. 6). Moreover, we observed that the joint effect of warming and nutrient enrichment significantly increased phytoplankton abundance as indicated by Chl *a* (Supporting Information Table S5), GPP, ER, NPP (table 2 in Ren et al. 2017), as well as bacterial production rates (Supporting Information Fig. S7, Fig. 6). The combination of warming and nutrient enrichment increased the autotrophic carbon supply and the heterotrophic carbon demand and led to changed carbon accumulation in the experimental shallow lakes.

The combination of warming and nutrient enrichment stimulated GPP (table 2 in Ren et al. 2017). In our study, potentially greater degrees of photoautotrophy and chemoautotrophy of bacteria were indicated in the nutrient-warming mesocosms by the higher relative abundances of photoautotrophic bacteria and chemolithotrophic bacteria with functional forms I and II of rubisco (Wang et al. 2009; Chan et al. 2013). High GPP in warm eutrophic mesocosms would increase the coupling between phytoplankton and the microbial community and lead to metabolization and recycling of a high proportion of the total photosynthesized organic matter by heterotrophic microorganisms. This suggestion is confirmed both by the higher bacterial biomass (Özen et al. 2013) and the higher bacterial production rates (Supporting Information Fig. S7) in the warming and nutrient-enriched mesocosms than in the controls. The production of organic matter by phytoplankton and the subsequent consumption by

Table 2. Major topological properties of the observed correlation-based networks and their associated random networks.

	Control		EW		NE		NE and EW	
Parameter	Observed	Random	Observed	Random	Observed	Random	Observed	Random
No. of genes	3236		3796		4151		2752	
No. of nodes	2843	2843	3328	3328	3649	3649	2543	2543
No. of edges	51,807	51,807	59,682	59,682	62,242	62,242	58,370	58,370
R^2	0.838	0.018	0.838	0.019	0.838	0.027	0.830	0.074
Clustering coefficient	0.403	0.013	0.405	0.011	0.414	0.009	0.437	0.018
Betweenness centrality	0.007	0.001	0.010	0.000	0.010	0.000	0.004	0.001
Closeness centrality	0.192	0.384	0.171	0.376	0.208	0.369	0.212	0.415
Average degree	36.445	36.445	35.867	35.867	34.115	34.115	45.906	45.906
Network centralization	0.086	0.007	0.081	0.006	0.073	0.005	0.104	0.008
Network density	0.013	0.013	0.011	0.011	0.009	0.009	0.018	0.018
Characteristic path length	6.312	2.606	7.706	2.661	6.962	2.711	6.142	2.411
Network heterogeneity	1.372	0.162	1.46	0.165	1.473	0.167	1.282	0.147
Connected components	33	1	52	1	65	1	14	1
Neighborhood connectivity	50.803	37.405	49.844	36.844	46.978	35.066	63.179	46.900
Number of directed edges	36.445	36.445	35.867	35.867	34.115	34.115	45.906	45.906
Average shortest path length	6.054	2.606	7.285	2.661	6.224	2.711	5.724	2.411
Copresence links	51,807		59,681		62,223		58,369	
Exclusion links	0		1		19		1	
Copresence links/total links	1.000		1.000		1.000		1.000	

heterotrophic microorganisms are very important processes for the carbon flux in shallow ecosystems. In this study, we observed that the microbial carbon degradation potentials increased significantly under the combined effects of warming and nutrient enrichment. However, we observed a net increase in carbon accumulation under the joint effect of warming and nutrient enrichment. The different temperature sensitivities of food web components may cause a loss of synchrony between the autotrophic carbon supply and the heterotrophic carbon demand, as predicted by the "match–mismatch" theory (Edwards and Richardson 2004). The coupling between C fixation by phytoplankton and organic C utilization by heterotrophic microorganisms may differ with respect to relative timing during spring. For the lag time between autotrophic C fixation and heterotrophic C utilization, dead phytoplankton may be lost by sinking, leading to a reduction in substrates for microbial degradation in the water column and net carbon accumulation (Hoppe et al. 2008). In addition to the biological carbon pump, the net carbon accumulation in the warming and nutrient-enriched mesocosms might also be caused by the microbial carbon pump because of the microbial transformation of organic carbon from labile to recalcitrant states (Jiao and Zheng 2011).

The nitrogen and phosphorous cycles catalyzed by microbial communities are important biogeochemical cycles in eutrophic shallow lakes, but our knowledge about the underlying processes is still insufficient (Jeppesen et al. 2009). In our nutrient-enriched mesocosms, water nitrogen and phosphorous, both being important limiting nutrients for eutrophication, were enriched by the addition of $Ca(NO_3)_2$ and Na_2HPO_4 solutions, maintaining a constant loading of 54 mg P and 538 mg N in each mesocosm each week. High levels of nitrogen and phosphorus not only stimulated the growth of phytoplankton in the warming mesocosms but also increased water DO concentrations by photosynthesis. Most likely due to the increased water DO concentration in the nutrient-warming mesocosms, high nitrate enrichment did not result in an increased metabolic potential for denitrification and thus no potential increase in N_2O emission from the water column during the sampling time. However, high water DO and nitrate concentrations might explain the decreased metabolic potential for ammonification (gdh and ureC) and, in certain gene groups, for dissimilatory N reduction (nrfA). Similar results have been found in previous studies (Seitzinger et al. 2000; McCrackin and Elser 2010). As nitrate is an important nutrient for eukaryotic phytoplankton and acts as a key electron acceptor for microorganisms, it can be directly absorbed by eukaryotic phytoplankton as well as autotrophic and heterotrophic microorganisms for growth. Accordingly, we observed nitrate concentrations to be lower in the nutrient-warming mesocosms than in the nutrient-enriched mesocosms at ambient temperature (Supporting Information Table S5).

Under phosphate-enriched conditions, phosphate might intermittently accumulate and be buried in the sediment (Søndergaard et al. 2001; Feuchtmayr et al. 2009; Ren

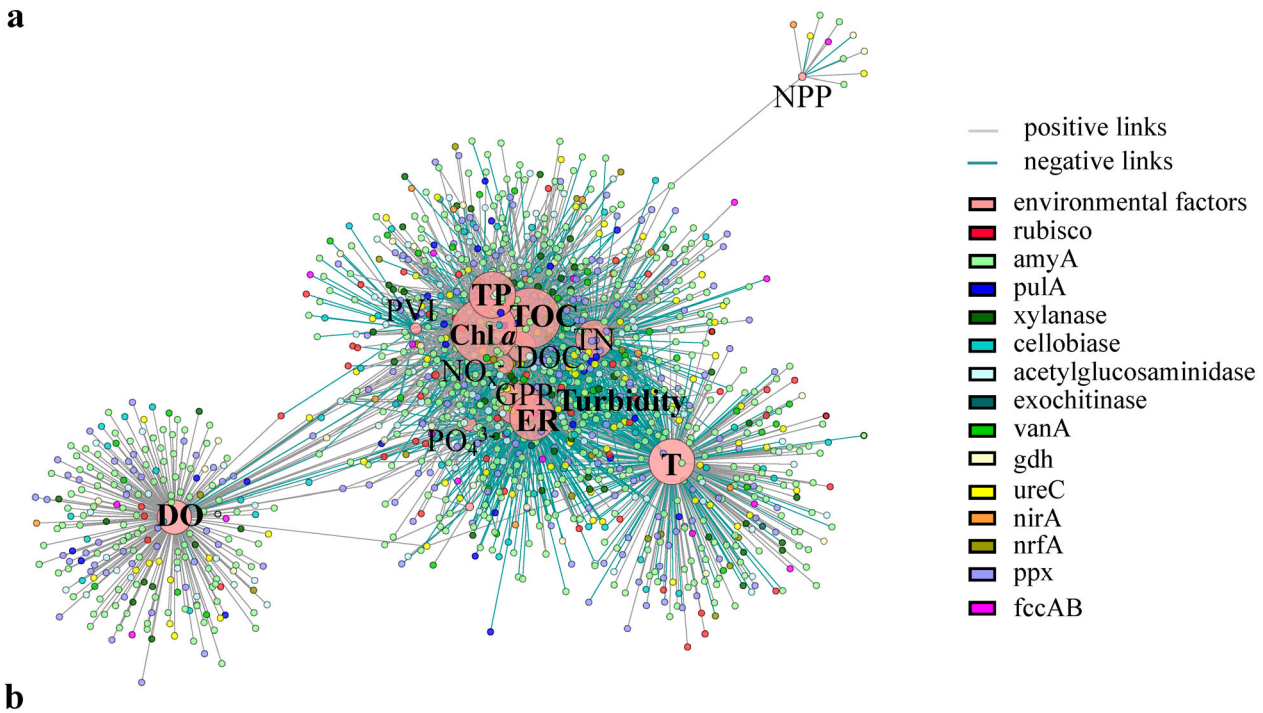

b

Environmental factors	Chl *a*	TOC	TP	GPP	T	ER	turbidity	DO	DOC	TN	NO_x^-	PVI	PO_4^{3-}	NPP
Degree	518	472	353	347	346	333	274	244	199	107	70	44	15	11

Fig. 5. Co-occurring network (**a**) showing the relationships between the characteristics of the water environment and ecosystem metabolism factors and the key gene groups involved in the biogeochemical cycling processes of carbon (rubisco, amyA, pulA, xylanase, cellobiase, acetylglucosaminidase, exochitinase, and vanA), nitrogen (gdh, ureC, nirA, and nrfA), phosphorus (ppx), and sulfur cycling (i.e., fccAB). Significant positive (gray) and negative (blue) relations were kept. The degree of each environmental factor is given in the table (**b**).

et al. 2018). The availability of phosphorus in many aquatic habitats inhabited by plankton is therefore scarce and/or fluctuating. Most microorganisms, including cyanobacteria, have several acclimation strategies to deal with phosphorus limitation as well as the ability to store phosphorus (Grossman et al. 1994). Previous studies found that polyphosphate (polyP) can be accumulated when the phosphate influx into the cell is larger than its current metabolic demand. Microorganisms can store phosphate in the form of polyP to very high intracellular concentrations ranging from μmol L^{-1} to mmol L^{-1}, when phosphate is available in excess (Rao et al. 2009; Li et al. 2020). PolyP is synthesized in microorganisms by polyphosphate kinase, encoded by ppk, and degraded by exopolyphosphatases, encoded by ppx (Hirota et al. 2010; Ren et al. 2018). This accumulated polyP can contribute to survival in the stationary phase, inhibition of RNA degradation, storage of energy, and regulation under stress and can also serve as a reservoir for inorganic phosphate (Sanz-Luque et al. 2020). Our results showed that the combination of warming and nutrient enrichment increased the metabolic potential for biosynthesis of polyP (ppk), suggesting that warming and nutrient enrichment in combination may stimulate phosphorous use by microorganisms and enhance the intracellular accumulation of polyP, which may increase the storage of inorganic phosphate and inhibit phosphate burial in sediments. In addition, probably due to the increased demand for inorganic phosphate, the metabolic potential for polyphosphate degradation (ppx) increased noticeably under the joint effect of warming and nutrient enrichment. The phosphate released from polyphosphate might lead to expansion of phytoplankton/microorganisms under phosphate-deficient conditions (Vadstein 2000; Bai et al. 2009) and might contribute to a higher phytoplankton/microorganism biomass as observed under the combined effects of warming and nutrient enrichment (Supporting Information Table S5 and Fig. S7). However, higher temperature-induced internal phosphorous loading might also contribute to the higher phytoplankton/microorganism biomass in the treatment of warming and nutrient enrichment, as seen in several other investigations (e.g., Jensen and Andersen 1992; Søndergaard et al. 2003).

The combination of warming and nutrient addition not only altered the microbial functional potentials for the nutrient cycling of C, N, and P but also significantly changed the

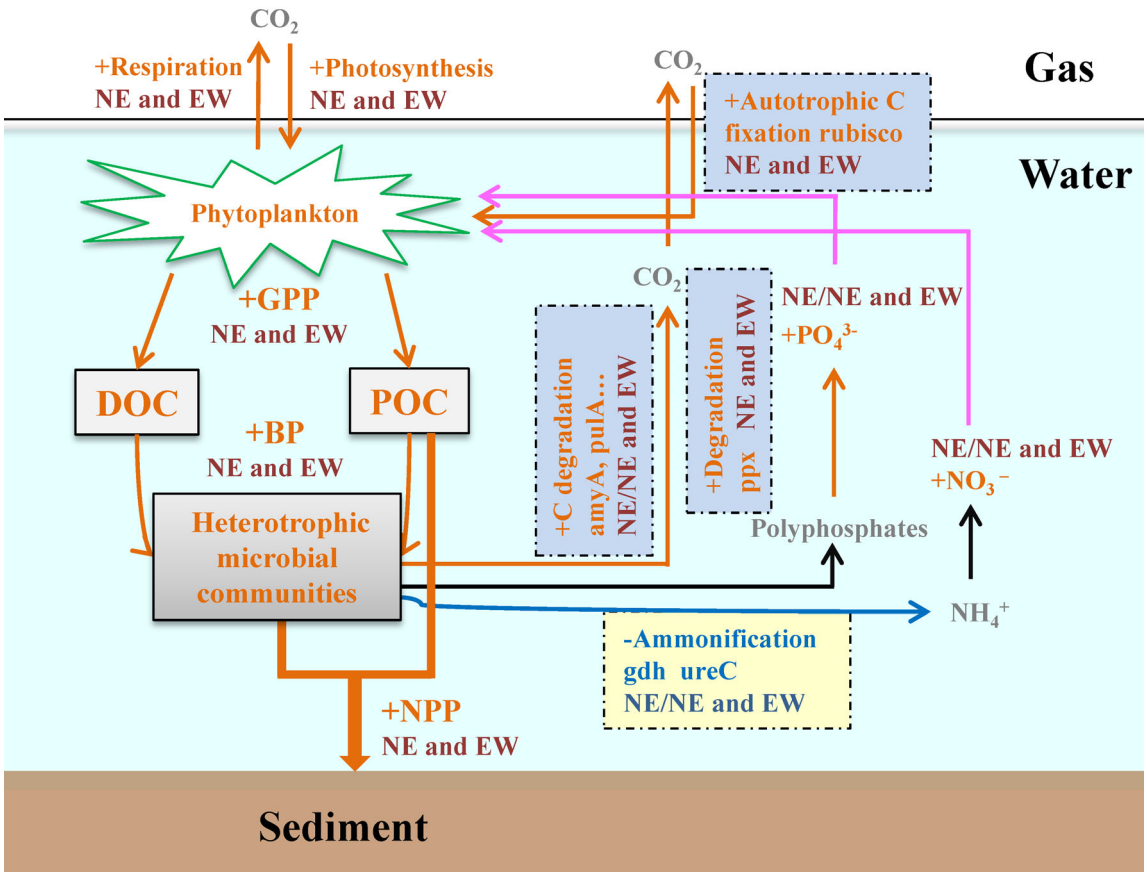

Fig. 6. A conceptual model of the microbial metabolic processes in different warming and nutrient-enriched treatments. The impacts of both environmental parameters and microbial community processes are labeled by "+," "the orange font" and "the orange arrow" if stimulating effects in the treatments were observed and by "–," "the blue font" and "the blue arrow" if inhibiting effects in the treatments were found. Moreover, "the black arrow" means no significant differences of microbial community processes in the treatments, and "the gray font" represents the unmeasured environmental parameters in this study. Phosphates and nitrates that could be directly assimilated by phytoplankton are displayed by the purple arrows. NE: the pure effect of nutrient enrichment; NE and EW: the combined effect of nutrient enrichment and enhanced warming; NE/ NE and EW: both the pure effect of nutrient enrichment and the combined effect of nutrient enrichment and enhanced warming. POC, particulate organic carbon.

microbial functional structure and its underlying mechanisms. Both deterministic and stochastic processes contribute to microbial community assembly, but their relative importance can be regulated by environmental/ecological conditions (Cavender-Bares et al. 2009; Logares et al. 2013; Ren et al. 2018). We found that warming and nutrient conditions, like other water environmental factors (e.g., pH, Ren et al. 2018), were capable of regulating microbial functional assembly processes. The relative importance of deterministic processes significantly increased under the combined effect of warming and nutrient enrichment. It is not surprising that the deterministic processes played a more important role in shaping the microbial functional gene assembly in the warming and nutrient-enriched mesocosms than in the other treatments. We found that Chl *a*, an indicator of phytoplankton abundance, was the key determiner shaping the microbial functional gene assembly. The input of nitrogen and phosphorus significantly and substantially increased the abundance of phytoplankton in the warming mesocosms (Supporting Information Table S5). High prevalence of phytoplankton often reduces local habitat availability (Eiler and Bertilsson 2004; Dziallas and Grossart 2011; Jankowski et al. 2014; Filiz et al. 2020) and increases the coupling of phytoplankton–microorganisms dynamics (Teeling et al. 2012, 2016), resulting in a strong deterministic effect on the microbial functional structure in the surrounding water (Romera-Castillo et al. 2011; Buchan et al. 2014; Penn et al. 2014; Yang et al. 2016).

The increased deterministic effect of phytoplankton was confirmed by network analysis. We observed that under the combination of warming and nutrient enrichment, the components, heterogeneity, as well as the shortest distance of the correlation-based network decreased significantly, while the network clustering coefficient, the degree, the density, as well as the connectivity increased significantly in comparison with other treatments. The higher interlinking of microbial

functional genes involved in the nutrient cycling of C, N, P, and S was probably caused by the enhanced deterministic processes from phytoplankton under the combined warming and nutrient enrichment. Although N, P, and S are not directly part of the biochemical process of phytoplankton production, essential macronutrients are required by primary producers to generate biomolecules such as proteins, nucleotides, and lipids (Litchman et al. 2015). Therefore, the production of phytoplankton is important in coupling C to N, P, or S in aquatic ecosystems (Martiny et al. 2013; Litchman et al. 2015). Moreover, under the combined effect of warming and nutrient enrichment, the increased coupling of the production of organic matter by phytoplankton and the subsequent consumption by heterotrophic bacteria may contribute to the interactions of C, N, P, and S cycling (Van den Meersche et al. 2004), resulting in the higher interlinking of microbial functional genes involved in the nutrient cycling of C, N, P, and S in the warming and nutrient-enriched treatment.

Conclusions

Our results showed that warming exacerbated the impact of nutrient enrichment on microbial metabolic potentials in our experiment conducted at the beginning of April. The joint effects of warming and nutrient enrichment significantly increased the microbial functional potentials in carbon fixation and degradation. The polyphosphate mobilization potential of microorganisms also increased significantly due to the joint effect of warming and nutrient enrichment. We also observed that warming enhanced the nutrient enrichment impacts on the microbial functional gene structure. The combination of warming and nutrient enrichment increased the deterministic processes and caused higher interlinking of microbial functional genes involved in the C, N, P, and S cycling in the correlation-based network. Overall, we propose that the joint effect of warming and nutrient enrichment altered the autotrophic carbon supply and the heterotrophic carbon demand and changed the carbon fluxes recorded in the experimental mesocosms. Our study that conducted at the beginning of April demonstrated a remarkable impact of warming on the microbial functional gene structure in the nutrient-enriched freshwater mesocosms and confirmed the potential feedbacks of microbial communities to warming in experimental shallow lakes. These observations may help to recognize the potential importance of microbial functional response in climate change biology.

Data availability statement

The GeoChip 5.0 data set is available in the Gene Expression Omnibus repository with the accession number GSE155582 (www.ncbi.nlm.nih.gov/geo/). Environmental variables and ecosystem functioning data used are available from the corresponding author upon reasonable request.

References

Allison, S. D., and J. B. Martiny. 2008. Resistance, resilience, and redundancy in microbial communities. Proc. Natl. Acad. Sci. USA **105**: 11512–11519. doi:10.1073/pnas.0801925105

Assenov, Y., F. Ramírez, S. E. Schelhorn, T. Lengauer, and M. Albrecht. 2008. Computing topological parameters of biological networks. Bioinformatics **24**: 282–284. doi:10.1093/bioinformatics/btm554

Bai, X., S. Ding, C. Fan, T. Liu, D. Shi, and L. Zhang. 2009. Organic phosphorus species in surface sediments of a large, shallow, eutrophic lake, Lake Taihu, China. Environ. Pollut. **157**: 2507–2513. doi:10.1016/j.envpol.2009.03.018

Barberán, A., A. Fernández-Guerra, B. J. M. Bohannan, and E. O. Casamayor. 2012. Exploration of community traits as ecological markers in microbial metagenomes. Mol. Ecol. **21**: 1909–1917. doi:10.1111/j.1365-294X.2011.05383.x

Bell, T., J. A. Newman, B. W. Silverman, S. L. Turner, and A. K. Lilley. 2005. The contribution of species richness and composition to bacterial services. Nature **436**: 1157–1160. doi:10.1038/nature03891

Brown, J. H., J. F. Gillooly, A. P. Allen, V. M. Savage, and G. B. West. 2004. Toward a metabolic theory of ecology. Ecology **85**: 1771–1789. doi:10.1890/03-9000

Buchan, A., G. R. LeCleir, C. A. Gulvik, and J. M. González. 2014. Master recyclers: Features and functions of bacteria associated with phytoplankton blooms. Nat. Rev. Microbiol. **12**: 686–698. doi:10.1038/nrmicro3326

Cavender-Bares, J., K. H. Kozak, P. V. Fine, and S. W. Kembel. 2009. The merging of community ecology and phylogenetic biology. Ecol. Lett. **12**: 693–715. doi:10.1111/j.1461-0248.2009.01314.x

Cavicchioli, R., and others. 2019. Scientists' warning to humanity: Microorganisms and climate change. Nat. Rev. Microbiol. **17**: 569–586. doi:10.1038/s41579-019-0222-5

Chan, Y., J. D. Van Nostrand, J. Zhou, S. B. Pointing, and R. L. Farrell. 2013. Functional ecology of an Antarctic Dry Valley. Proc. Natl. Acad. Sci. USA **110**: 8990–8995. doi:10.1073/pnas.1300643110

Christoffersen, K., N. Andersen, M. Søndergaard, L. Liboriussen, and E. Jeppesen. 2006. Implications of climate-enforced temperature increases on freshwater pico- and nanoplankton populations studied in artificial ponds during 16 months. Hydrobiologia **560**: 259–266. doi:10.1007/s10750-005-1221-2

Davidson, T. A., J. Audet, E. Jeppesen, F. Landkildehus, T. L. Lauridsen, M. Søndergaard, and J. Syväranta. 2018. Synergy between nutrients and warming enhances methane ebullition from experimental lakes. Nat. Clim. Chang. **8**: 156–160. doi:10.1038/s41558-017-0063-z

Dziallas, C., and H. P. Grossart. 2011. Temperature and biotic factors influence bacterial communities associated with the cyanobacterium *Microcystis* sp. Environ. Microbiol. **13**: 1632–1641. doi:10.1111/j.1462-2920.2011.02479.x

Edwards, M., and A. J. Richardson. 2004. Impact of climate change on marine pelagic phenology and trophic mismatch. Nature **430**: 881–884. doi:10.1038/nature02808

Eiler, A., and S. Bertilsson. 2004. Composition of freshwater bacterial communities associated with cyanobacterial blooms in four Swedish lakes. Environ. Microbiol. **6**: 1228–1243. doi:10.1111/j.1462-2920.2004.00657.x

Escalas, A., L. Hale, J. W. Voordeckers, Y. Yang, M. K. Firestone, L. Alvarez-Cohen, and J. Zhou. 2019. Microbial functional diversity: From concepts to applications. Ecol. Evol. **9**: 12000–12016. doi:10.1002/ece3.5670

Faust, K., and J. Raes. 2012. Microbial interactions: From networks to models. Nat. Rev. Microbiol. **10**: 538–550. doi:10.1038/nrmicro2832

Feuchtmayr, H., R. Moran, K. Hatton, L. Connor, T. Heyes, B. Moss, I. Harvey, and D. Atkinson. 2009. Global warming and eutrophication: Effects on water chemistry and autotrophic communities in experimental hypertrophic shallow lake mesocosms. J. Appl. Ecol. **46**: 713–723. doi:10.1111/j.1365-2664.2009.01644.x

Filiz, N., and others. 2020. Phytoplankton community response to nutrients, temperatures, and a heat wave in shallow lakes: An experimental approach. Water **12**: 3394. doi:10.3390/W12123394

Flanagan, K. M., E. McCauley, F. Wrona, and T. Prowse. 2003. Climate change: The potential for latitudinal effects on algal biomass in aquatic ecosystems. Can. J. Fish. Aquat. Sci. **60**: 635–639. doi:10.1139/f03-062

Fuhrman, J. A., and F. Azam. 1982. Thymidine incorporation as a measure of heterotrophic bacterioplankton in marine surface waters: Evalution and field results. Mar. Biol. **66**: 109–120. doi:10.1007/BF00397184

Garcia, S. L., and others. 2013. Metabolic potential of a single cell belonging to one of the most abundant lineages in freshwater bacterioplankton. ISME J. **7**: 137–147. doi:10.1038/ismej.2012.86

Grossman, A. R., D. Bhaya, and J. L. Collier. 1994. Specific and general responses of cyanobacteria to macronutrient deprivation, p. 112–118.*In* A. Torriani-Gorini, E. Yagil, and S. Silver [eds.], Phosphate in microorganisms. ASM Press.

Guo, X., and others. 2019. Climate warming accelerates temporal scaling of grassland soil microbial biodiversity. Nat. Ecol. Evol. **3**: 612–619. doi:10.1038/s41559-019-0848-8

He, Z., Y. Deng, and J. Zhou. 2012. Development of functional gene microarrays for microbial community analysis. Curr. Opin. Biotechnol. **23**: 49–55. doi:10.1016/j.copbio.2011.11.001

Hirota, R., A. Kuroda, J. Kato, and H. Ohtake. 2010. Bacterial phosphate metabolism and its application to phosphorus recovery and industrial bioprocesses. J. Biosci. Bioeng. **109**: 423–432. doi:10.1016/j.jbiosc.2009.10.018

Hoegh-Guldberg, O., and J. F. Bruno. 2010. The impact of climate change on the world's marine ecosystems. Science **328**: 1523–1528. doi:10.1126/science.1189930

Hoppe, H. G., P. Breithaupt, K. Walther, R. Koppe, S. Bleck, U. Sommer, and K. Jürgens. 2008. Climate warming in winter affects the coupling between phytoplankton and bacteria during the spring bloom: A mesocosm study. Aquat. Microb. Ecol. **51**: 105–115. doi:10.3354/ame01198

IPCC. 2007. R. K. Pachauri and A. Reisinger Climate Change 2007: Synthesis Report. Contribution of Working Groups I, II and III to the Fourth Assessment Report of the Intergovernmental Panel on Climate Change. Geneva, Switzerland: IPCC. https://www.ipcc.ch/report/ar4/syr/.

Jankowski, K., D. E. Schindler, and M. C. Horner-Devine. 2014. Resource availability and spatial heterogeneity control bacterial community response to nutrient enrichment in lakes. PLoS One **9**: e86991. doi:10.1371/journal.pone.0086991

Jensen, H. S., and F. O. Andersen. 1992. Importance of temperature, nitrate, and pH for phosphate release from aerobic sediments of four shallow, eutrophic lakes. Limnol. Oceanogr. **37**: 577–589. doi:10.4319/lo.1992.37.3.0577

Jeppesen, E., and others. 2009. Climate change effects on runoff, catchment phosphorus loading and lake ecological state, and potential adaptations. J. Environ. Qual. **38**: 1930–1941. doi:10.2134/jeq2008.0113

Jeppesen, E., and others. 2010. Chapter 6: Interaction of climate change and eutrophication, p. 119–151.*In* M. Kernan, R. Battarbee, and B. Moss [eds.], Changing climate and changing freshwaters: A European perspective. Blackwell.

Jiao, N., and Q. Zheng. 2011. The microbial carbon pump: From genes to ecosystems. Appl. Environ. Microbiol. **77**: 7439–7444. doi:10.1128/AEM.05640-11

Kelly, L. W., and others. 2019. Diel population and functional synchrony of microbial communities on coral reefs. Nat. Commun. **10**: 1–9. doi:10.1038/s41467-019-09419-z

Kiersztyn, B., R. Chróst, T. Kaliński, W. Siuda, A. Bukowska, G. Kowalczyk, and K. Grabowska. 2019. Structural and functional microbial diversity along a eutrophication gradient of interconnected lakes undergoing anthropopressure. Sci. Rep. **9**: 1–14. doi:10.1038/s41598-019-47577-8

Kosten, S., E. Jeppesen, V. L. Huszar, N. Mazzeo, E. H. van Nes, E. T. Peeters, and M. Scheffer. 2011. Ambiguous climate impacts on competition between submerged macrophytes and phytoplankton in shallow lakes. Freshw. Biol. **56**: 1540–1553. doi:10.1111/j.1365-2427.2011.02593.x

Kumar, S., G. Stecher, M. Li, C. Knyaz, and K. Tamura. 2018. MEGA X: Molecular evolutionary genetics analysis across computing platforms. Mol. Biol. Evol. **35**: 1547–1549. doi:10.1093/molbev/msy096

Legendre, P., and L. Legendre. 2012. Numerical ecology. Amsterdam: Elsevier.

Li, H., M. Barber, J. Lu, and R. Goel. 2020. Microbial community successions and their dynamic functions during harmful cyanobacterial blooms in a freshwater lake. Water Res. **185**: 116292. doi:10.1016/j.watres.2020.116292

Liboriussen, L., and others. 2005. Global warming: Design of a flow-through shallow lake mesocosm climate experiment.

Limnol. Oceanogr.: Methods **3**: 1–9. doi:10.4319/lom.2005.3.1

Litchman, E., P. de Tezanos Pinto, K. F. Edwards, C. A. Klausmeier, C. T. Kremer, and M. K. Thomas. 2015. Global biogeochemical impacts of phytoplankton: A trait-based perspective. J. Ecol. **103**: 1384–1396. doi:10.1111/1365-2745.12438

Logares, R., and others. 2013. Biogeography of bacterial communities exposed to progressive long-term environmental change. ISME J. **7**: 937–948. doi:10.1038/ismej.2012.168

Love, M. I., W. Huber, and S. Anders. 2014. Moderated estimation of fold change and dispersion for RNA-seq data with DESeq2. Genome Biol. **15**: 550. doi:10.1186/s13059-014-0550-8

Martiny, A. C., C. T. Pham, F. W. Primeau, J. A. Vrugt, J. K. Moore, S. A. Levin, and M. W. Lomas. 2013. Strong latitudinal patterns in the elemental ratios of marine plankton and organic matter. Nat. Geosci. **6**: 279–283. doi:10.1038/ngeo1757

McCrackin, M. L., and J. J. Elser. 2010. Atmospheric nitrogen deposition influences denitrification and nitrous oxide production in lakes. Ecology **91**: 528–539. doi:10.1890/08-2210.1

Meerhoff, M., J. M. Clemente, F. T. de Mello, C. Iglesias, A. R. Pedersen, and E. Jeppesen. 2007. Can warm climate-related structure of littoral predator assemblies weaken the clear water state in shallow lakes? Glob. Chang. Biol. **13**: 1888–1897. doi:10.1111/j.1365-2486.2007.01408.x

O'Connor, M. I., M. F. Piehler, D. M. Leech, A. Anton, and J. F. Bruno. 2009. Warming and resource availability shift food web structure and metabolism. PLoS Biol. **7**: e1000178. doi:10.1371/journal.pbio.1000178

Özen, A., and others. 2013. Long-term effects of warming and nutrients on microbes and other plankton in mesocosms. Freshw. Biol. **58**: 483–493. doi:10.1111/j.1365-2427.2012.02824.x

Penn, K., J. Wang, S. C. Fernando, and J. R. Thompson. 2014. Secondary metabolite gene expression and interplay of bacterial functions in a tropical freshwater cyanobacterial bloom. ISME J. **8**: 1866–1878. doi:10.1038/ismej.2014.27

Posch, T., O. Köster, M. M. Salcher, and J. Pernthaler. 2012. Harmful filamentous cyanobacteria favoured by reduced water turnover with lake warming. Nat. Clim. Chang. **2**: 809–813. doi:10.1038/nclimate1581

Rao, N. N., M. R. Gomez-Garcia, and A. Kornberg. 2009. Inorganic polyphosphate: Essential for growth and survival. Annu. Rev. Biochem. **78**: 605–647. doi:10.1146/annurev.biochem.77.083007.093039

Ren, L., D. He, Z. Chen, E. Jeppesen, T. L. Lauridsen, M. Søndergaard, Z. Liu, and Q. L. Wu. 2017. Warming and nutrient enrichment in combination increase stochasticity and beta diversity of bacterioplankton assemblages across freshwater mesocosms. ISME J. **11**: 613–625. doi:10.1038/ismej.2016.159

Ren, L., X. Song, E. Jeppesen, P. Xing, L. Liboriussen, X. Xu, and Q. L. Wu. 2018. Contrasting patterns of freshwater microbial metabolic potentials and functional gene interactions between an acidic mining lake and a weakly alkaline lake. Limnol. Oceanogr. **63**: S354–S366. doi:10.1002/lno.10744

Rigosi, A., C. C. Carey, B. W. Ibelings, and J. D. Brookes. 2014. The interaction between climate warming and eutrophication to promote cyanobacteria is dependent on trophic state and varies among taxa. Limnol. Oceanogr. **59**: 99–114. doi:10.4319/lo.2014.59.1.0099

Roh, S. W., G. C. Abell, K. H. Kim, Y. D. Nam, and J. W. Bae. 2010. Comparing microarrays and next-generation sequencing technologies for microbial ecology research. Trends Biotechnol. **28**: 291–299. doi:10.1016/j.tibtech.2010.03.001

Romera-Castillo, C., H. Sarmento, X. A. Alvarez-Salgado, J. M. Gasol, and C. Marrasé. 2011. Net production and consumption of fluorescent colored dissolved organic matter by natural bacterial assemblages growing on marine phytoplankton exudates. Appl. Environ. Microbiol. **77**: 7490–7498. doi:10.1128/AEM.00200-11

Sanz-Luque, E., D. Bhaya, and A. R. Grossman. 2020. Polyphosphate: A multifunctional metabolite in cyanobacteria and algae. Front. Plant Sci. **11**: 938. doi:10.3389/fpls.2020.00938

Seitzinger, S. P., C. Kroeze, and R. V. Styles. 2000. Global distribution of N_2O emissions from aquatic systems: Natural emissions and anthropogenic effects. Chemosphere Glob. Chang. Sci. **2**: 267–279. doi:10.1016/S1465-9972(00)00015-5

Shi, Z., and others. 2019. Functional gene array-based ultrasensitive and quantitative detection of microbial populations in complex communities. mSystems **4**: e00296-19. doi:10.1128/mSystems.00296-19

Shurin, J. B., J. L. Clasen, H. S. Greig, P. Kratina, and P. L. Thompson. 2012. Warming shifts top-down and bottom-up control of pond food web structure and function. Philos. Trans. R. Soc. Lond. B Biol. Sci. **367**: 3008–3017. doi:10.1098/rstb.2012.0243

Søndergaard, M., E. Jeppesen, E. Mortensen, E. Dall, P. Kristensen, and O. Sortkjær. 1990. Phytoplankton biomass reduction after planktivorous fish reduction in a shallow, eutrophic lake: A combined effect of reduced internal P-loading and increased zooplankton grazing. Hydrobiologia **200**: 229–240. doi:10.1007/BF02530342

Søndergaard, M., P. J. Jensen, and E. Jeppesen. 2001. Retention and internal loading of phosphorus in shallow, eutrophic lakes. ScientificWorldJournal **1**: 427–442. doi:10.1100/tsw.2001.72

Søndergaard, M., J. P. Jensen, and E. Jeppesen. 2003. Role of sediment and internal loading of phosphorus in shallow lakes. Hydrobiologia **506**: 135–145. doi:10.1023/B:HYDR.0000008611.12704.dd

Suenaga, H. 2012. Targeted metagenomics: A high-resolution metagenomics approach for specific gene clusters in complex microbial communities. Environ. Microbiol. **14**: 13–22. doi:10.1111/j.1462-2920.2011.02438.x

Teeling, H., and others. 2012. Substrate-controlled succession of marine bacterioplankton populations induced by a phytoplankton bloom. Science **336**: 608–611. doi:10.1126/science.1218344

Teeling, H., and others. 2016. Recurring patterns in bacterioplankton dynamics during coastal spring algae blooms. Elife **5**: e11888. doi:10.7554/eLife.11888.001

Vadstein, O. 2000. Heterotrophic, planktonic bacteria and cycling of phosphorus, p. 115–167.*In* B. Schink [ed.], Advances in microbial ecology. Springer.

Van den Meersche, K., J. J. Middelburg, K. Soetaert, P. Van Rijswijk, H. T. Boschker, and C. H. Heip. 2004. Carbon–nitrogen coupling and algal–bacterial interactions during an experimental bloom: Modeling a ^{13}C tracer experiment. Limnol. Oceanogr. **49**: 862–878. doi:10.4319/lo.2004.49.3.0862

Verpoorter, C., T. Kutser, D. A. Seekell, and L. J. Tranvik. 2014. A global inventory of lakes based on high-resolution satellite imagery. Geophys. Res. Lett. **41**: 6396–6402. doi:10.1002/2014GL060641

Wang, F., and others. 2009. GeoChip-based analysis of metabolic diversity of microbial communities at the Juan de Fuca Ridge hydrothermal vent. Proc. Natl. Acad. Sci. USA **106**: 4840–4845. doi:10.1073/pnas.0810418106

Woodward, G., D. M. Perkins, and L. E. Brown. 2010. Climate change and freshwater ecosystems: Impacts across multiple levels of organization. Philos. Trans. R. Soc. Lond. B Biol. Sci. **365**: 2093–2106. doi:10.1098/rstb.2010.0055

Wu, Q. L., G. Zwart, J. Wu, M. P. Kamst-van Agterveld, S. Liu, and M. W. Hahn. 2007. Submersed macrophytes play a key role in structuring bacterioplankton community composition in the large, shallow, subtropical Taihu Lake, China. Environ. Microbiol. **9**: 2765–2774. doi:10.1111/j.1462-2920.2007.01388.x

Yan, Q., and others. 2015. Impacts of the Three Gorges Dam on microbial structure and potential function. Sci. Rep. **5**: 8605. doi:10.1038/srep08605

Yang, C., and others. 2016. A comprehensive insight into functional profiles of free-living microbial community responses to a toxic *Akashiwo sanguinea* bloom. Sci. Rep. **6**: 34645. doi:10.1038/srep34645

Yvon-Durocher, G., A. P. Allen, D. Bastviken, R. Conrad, C. Gudasz, A. St-Pierre, N. Thanh-Duc, and P. A. del Giorgio. 2014. Methane fluxes show consistent temperature dependence across microbial to ecosystem scales. Nature **507**: 488–491. doi:10.1038/nature13164

Yvon-Durocher, G., C. J. Hulatt, G. Woodward, and M. Trimmer. 2017. Long-term warming amplifies shifts in the carbon cycle of experimental ponds. Nat. Clim. Chang. **7**: 209–213. doi:10.1038/nclimate3229

Zhang, W., and others. 2019. Marine biofilms constitute a bank of hidden microbial diversity and functional potential. Nat. Commun. **10**: 1–10. doi:10.1038/s41467-019-08463-z

Zhou, J., and others. 2012. Microbial mediation of carbon-cycle feedbacks to climate warming. Nat. Clim. Chang. **2**: 106–110. doi:10.1038/nclimate1331

Zuckerkandl, E., and L. Pauling. 1965. Evolutionary divergence and convergence in proteins. *In* V. Bryson and H. J. Vogel [eds.], Evolving genes and proteins, (pp. 97–166). Academic Press.

Acknowledgments

We are very grateful to Lissa Skov Hansen for her excellent work with the chemical analyses and Anne Mette Poulsen for English language assistance. We also acknowledge Qingyun Yan, Te Cao, Haijun Wang, Femke van Beersum, and Jia Guo for their assistance with the experiment and data analysis. This work was supported by National Science Foundation (91951000, 416210002, and 31870445), the Key Research Program of Frontier Science, CAS (QYZDJ-SSW-DQC030), State Key Laboratory of Lake Science and Environment (2018SKL007), the Second Tibetan Plateau Scientific Expedition and Research (STEP) program (2019QZKK0503), AQUACOSM (Network of Leading European AQUAtic MesoCOSM Facilities Connecting Mountains to Oceans from the Arctic to the Mediterranean), AQUACOSMplus, AnaEE Denmark (anaee.dk), as well as the Tübitak Outstanding Researcher Program (BIDEB 2232, project 118C250). Qinglong L. Wu, Erik Jeppesen, Torben L. Lauridsen, and Martin Søndergaard made contributions to the design of the work. Lijuan Ren, Erik Jeppesen, and Qinglong L. Wu performed the field investigation. Lijuan Ren, Yuanyuan Liu, and Jizhong Zhou performed sample and data analyses. Lijuan Ren, Boping Han, Erik Jeppesen, Jizhong Zhou, Jianjun Wang, and Qinglong L. Wu drafted and substantively revised the work.

Conflict of Interest

None declared.

Submitted 16 August 2020
Revised 20 March 2021
Accepted 26 March 2021

Associate editor: Hans-Peter Grossart